Title:

Specific Imaging of CD8+ T-Cell Dynamics with a Nanobody Radiotracer against Human CD8β

Journal:

European Journal of Nuclear Medicine and Molecular Imaging

Author information:

Authors

Timo W.M. De Groof[1,Δ,*], Yoline Lauwers[1,Δ], Tessa De Pauw[1], Mohit Saxena[2], Cécile Vincke[3,4], Jolien Van Craenenbroeck[3,4], Catherine Chapon[2], Roger Le Grand[2], Geert Raes[3,4], Thibaut Naninck[2], Jo A. Van Ginderachter[3,4,§] and Nick Devoogdt[1,§,*]

Affiliations

[1] Molecular Imaging and Therapy Laboratory, Vrije Universiteit Brussel, Brussels, Belgium
[2] Université Paris-Saclay, Inserm, CEA, Center for Immunology of Viral, Auto-immune, Hematological and Bacterial Diseases (IMVA-HB/IDMIT), Fontenay-aux-Roses & Le Kremlin-Bicêtre, Paris, France
[3] Laboratory of Myeloid Cell Immunology, VIB Center for Inflammation Research, Brussels, Belgium
[4] Brussels Center for Immunology, Vrije Universiteit Brussel, Brussels, Belgium
[Δ,§] These authors contributed equally
[*] Corresponding authors

Corresponding Authors:

Timo W.M. De Groof

Email: timo.de.groof@vub.be

Nick Devoogdt

Email: nick.devoogdt@vub.be

Supplemental Figures and tables

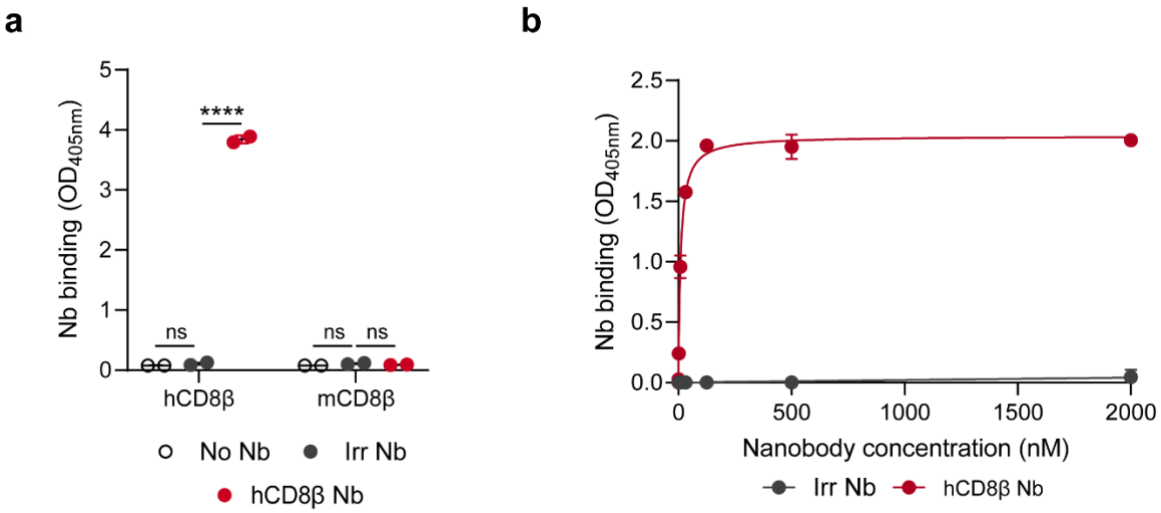

Supplemental Figure 1. Anti-human CD8β nanobody binds cynomolgus but not mouse CD8β protein. a) *Binding ELISA of irrelevant nanobody (Irr Nb) and anti-human CD8β nanobody (hCD8β Nb) to human (h) or mouse (m) CD8β protein.* ***b)*** *Binding ELISA of different concentrations of Irr Nb and hCD8β Nb to cynomolgus CD8β protein. Nb binding was detected using the C-terminal HA-tag and an anti HA-antibody. Data are shown as mean ± S.D.*

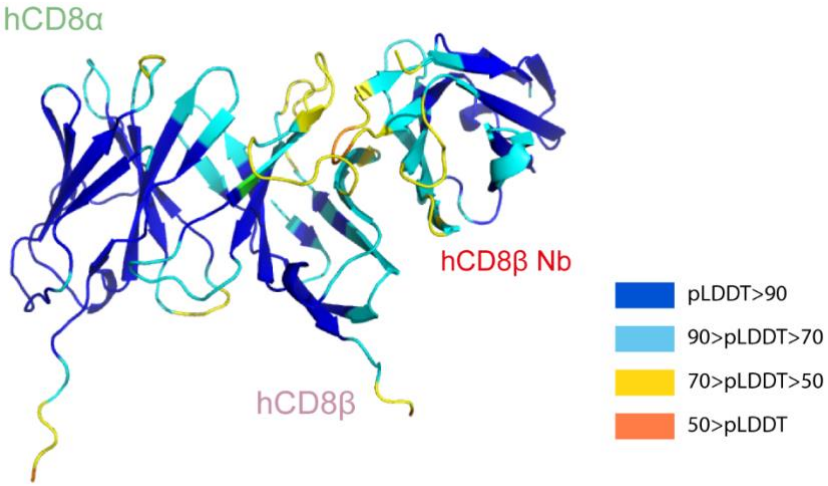

Supplemental Figure 2. Confidence model of the predicted Alphafold model. *pLDDT scores of the Alphafold prediction model of binding of anti-human CD8β nanobody (hCD8β Nb) to human CD8.*

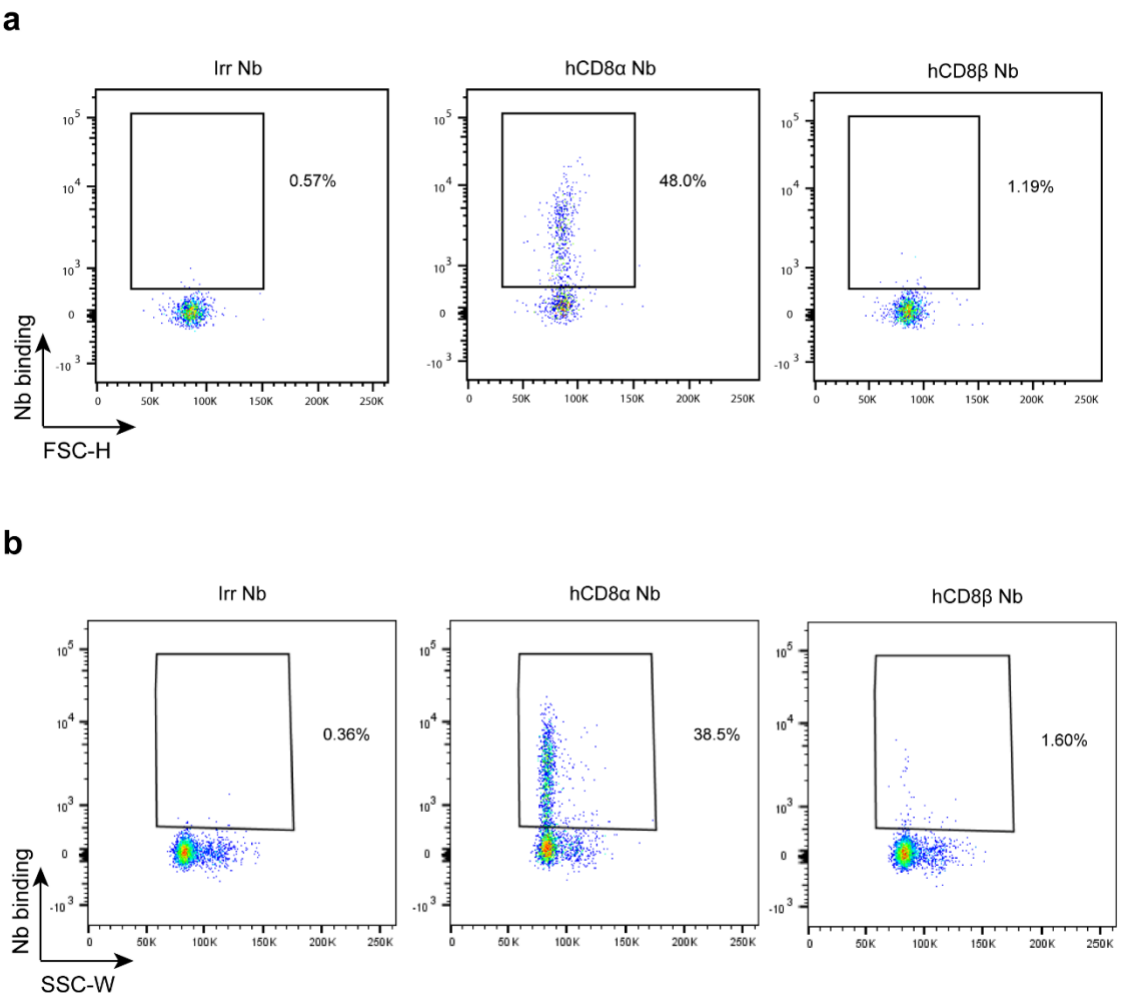

Supplemental Figure 3. Anti-human CD8β nanobody does not bind to NK or myeloid cells. *Binding of an irrelevant nanobody (Irr Nb), anti-human CD8α nanobody (hCD8α Nb) or anti-human CD8β nanobody (hCD8β Nb) to CD3$^-$ CD56$^+$ NK cells (**a**) or CD3$^-$ CD56$^-$ myeloid cells (**b**) obtained from a healthy donor. NK cells (CD45$^+$, CD19$^-$, CD3$^-$, CD56$^+$) or myeloid cells (CD45$^+$, CD19$^-$, CD3$^-$, CD56$^-$) were gated and Nb binding was detected via the C-terminal HA-tag and a fluorescently labeled anti-HA antibody.*

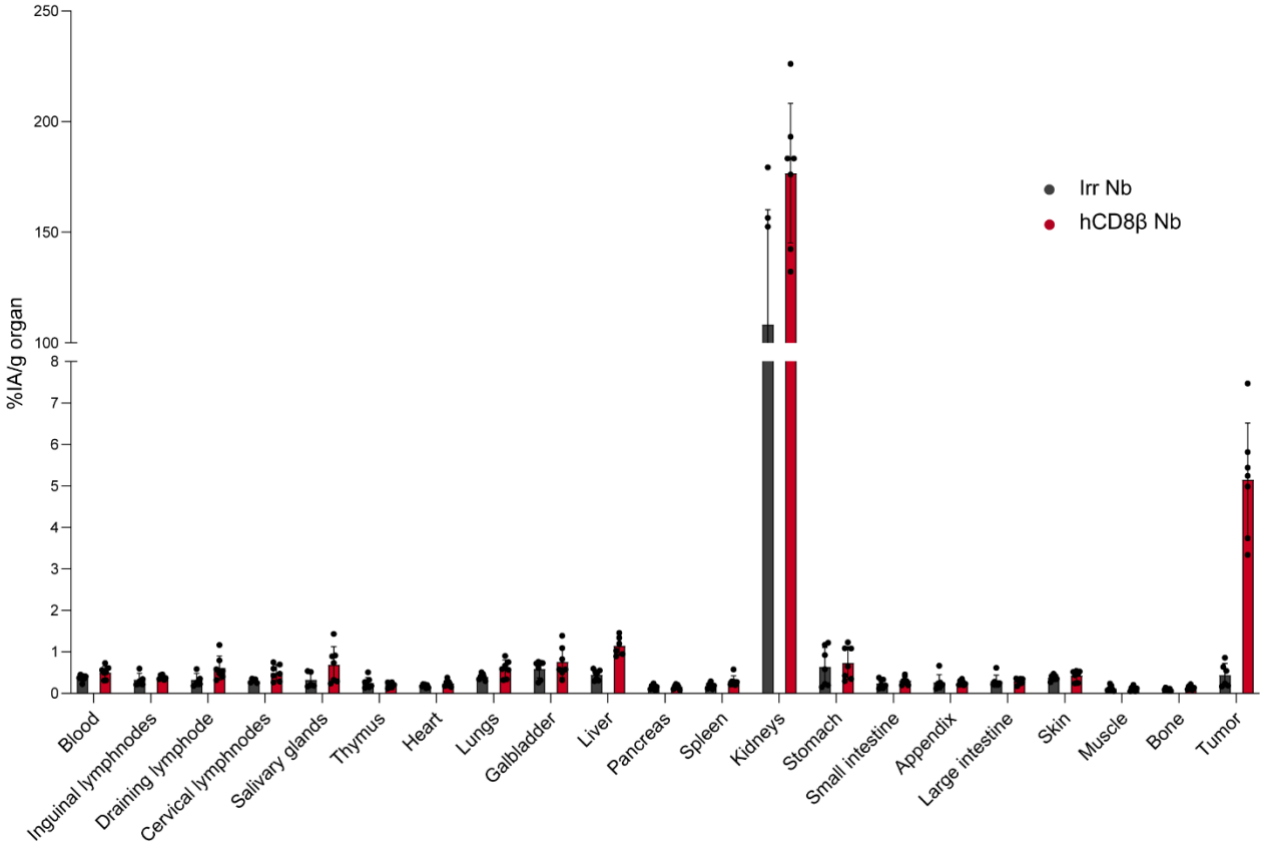

Supplemental Figure 4. Ex vivo biodistribution analysis of anti-human CD8β nanobody in SUP-T1 tumor bearing mice. *Ex vivo γ-counting of the isolated organs from SUP-T1 tumor-bearing nude mice 80min after injection with [^{99m}Tc]Tc-anti-human CD8β nanobody (hCD8β Nb) or [^{99m}Tc]Tc-irrelevant nanobody (Irr Nb). Biodistribution of the nanobodies in seven mice is shown and expressed as mean ± SD of percentage of injected activity per gram of organ or tissue (%IA/g).*

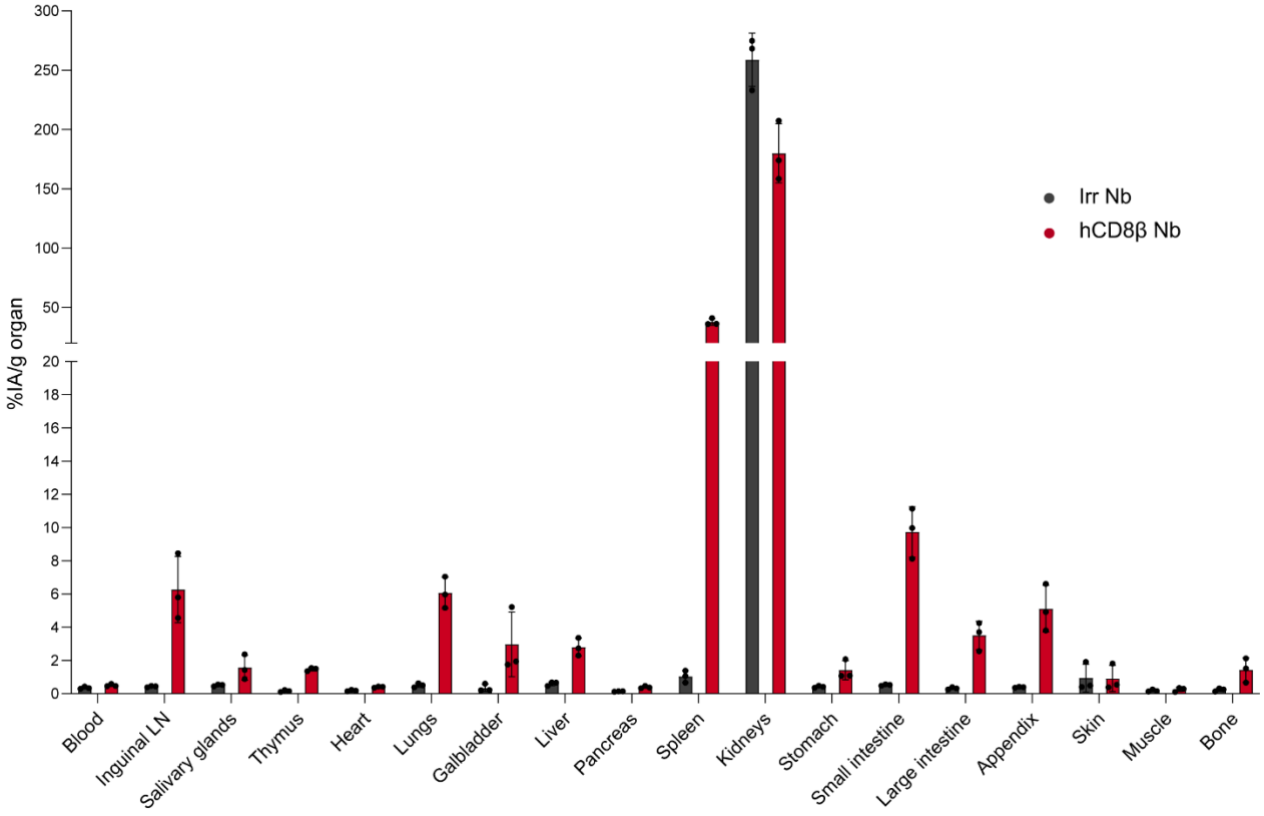

Supplemental Figure 5. Ex vivo biodistribution analysis of anti-human CD8β nanobody in naïve human CD8-transgenic mice. *Ex vivo γ-counting of the isolated organs from naïve human CD8-transgenic mice 80min after injection with [^{99m}Tc]Tc-anti-human CD8β nanobody (hCD8β Nb) or [^{99m}Tc]Tc-irrelevant nanobody (Irr Nb). Biodistribution of the nanobodies in three mice is shown and expressed as mean ± SD of percentage of injected activity per gram of organ or tissue (%IA/g).*

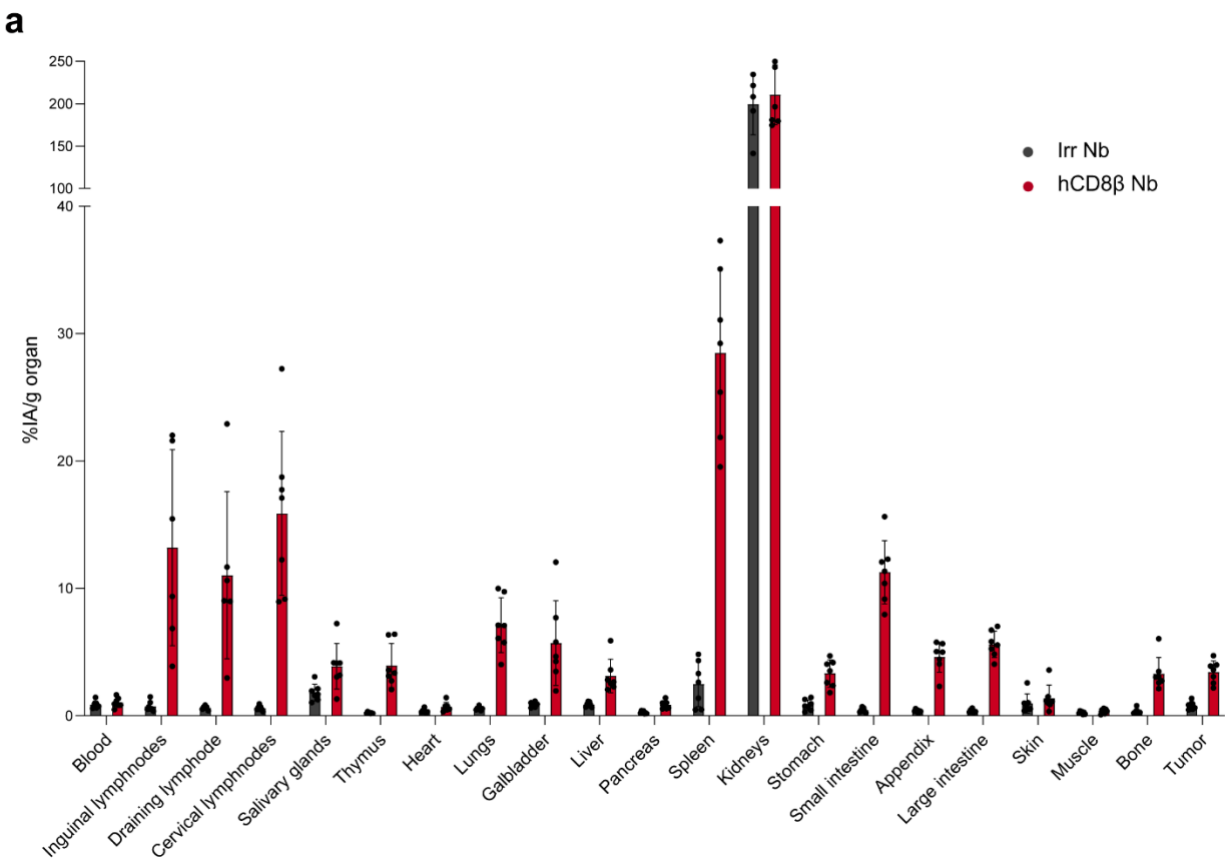
a
%IA/g organ
Irr Nb
hCD8β Nb
Blood
Inguinal lymphnodes
Draining lymphode
Cervical lymphnodes
Salivary glands
Thymus
Heart
Lungs
Gallbladder
Liver
Pancreas
Spleen
Kidneys
Stomach
Small intestine
Appendix
Large intestine
Skin
Muscle
Bone
Tumor

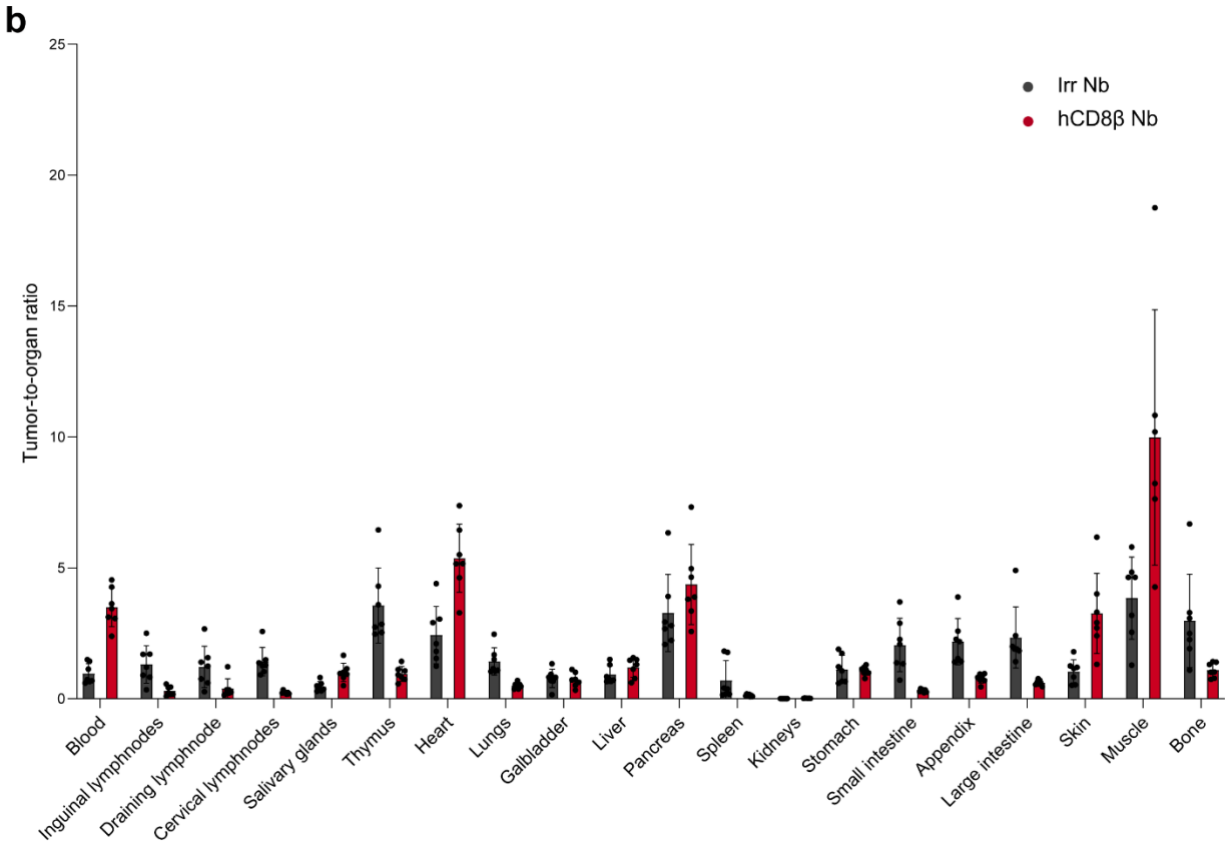
b
Tumor-to-organ ratio
Irr Nb
hCD8β Nb
Blood
Inguinal lymphnodes
Draining lymphode
Cervical lymphnodes
Salivary glands
Thymus
Heart
Lungs
Gallbladder
Liver
Pancreas
Spleen
Kidneys
Stomach
Small intestine
Appendix
Large intestine
Skin
Muscle
Bone

Supplemental Figure 6. Ex vivo biodistribution analysis of anti-human CD8β nanobody in MC38-tumor bearing human CD8-transgenic mice. *Ex vivo γ-counting (**a**) and tumor-to-organ ratios (**b**) of the isolated organs from MC38-tumor bearing human CD8-transgenic mice 80min after injection with [^{99m}Tc]Tc-anti-human CD8β nanobody (hCD8β Nb) or [^{99m}Tc]Tc-irrelevant nanobody (Irr Nb). Biodistribution and tumor-to-organ ratios of the nanobodies in seven mice are shown and expressed as mean ± SD of percentage of injected activity per gram of organ or tissue (%IA/g).*

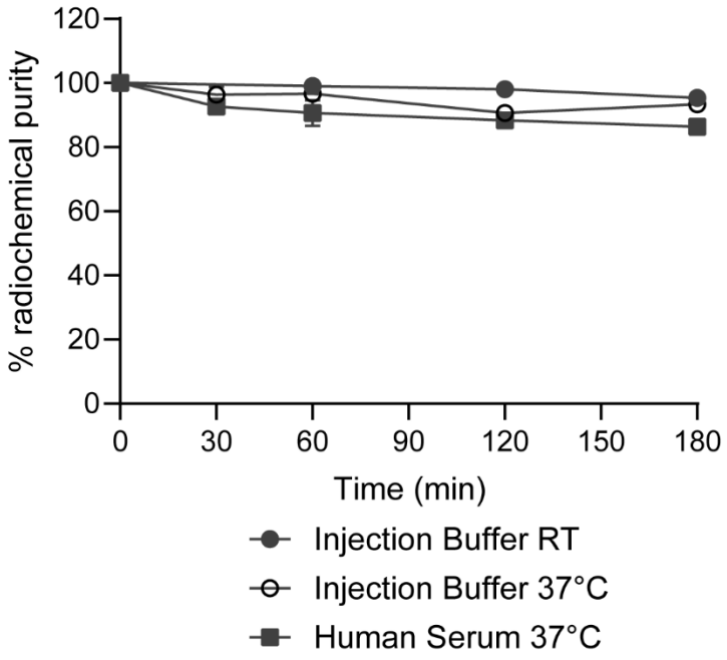

Supplemental Figure 7. [^{68}Ga]Ga-NOTA-anti-human CD8β nanobody is stable in injection buffer and in human serum. *Radiochemical purity of the [^{68}Ga]Ga-NOTA-anti-human CD8β nanobody in injection buffer (0.9% NaCl + 5mg/ml Vitamin C) at room temperature (RT), in injection buffer at 37°C, or in human serum. Purity is determined by radio-size exclusion chromatography and normalized to timepoint t=0.*

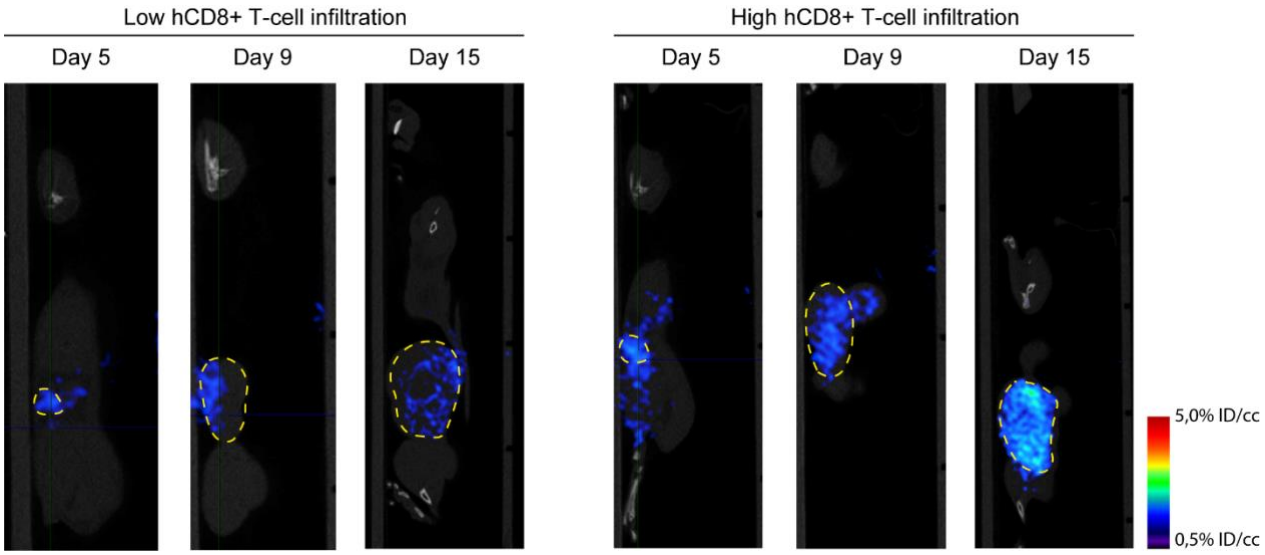

Supplemental Figure 8. PET/CT imaging of hCD8$^+$ T-cell infiltration with the [^{68}Ga]Ga-NOTA-anti-human CD8β nanobody. *Representative sagittal PET/CT image section of a MC38 tumor-bearing hCD8-transgenic mouse with low and high hCD8$^+$ intratumoral T-cell infiltration at different timepoints. The tumor is delineated.*

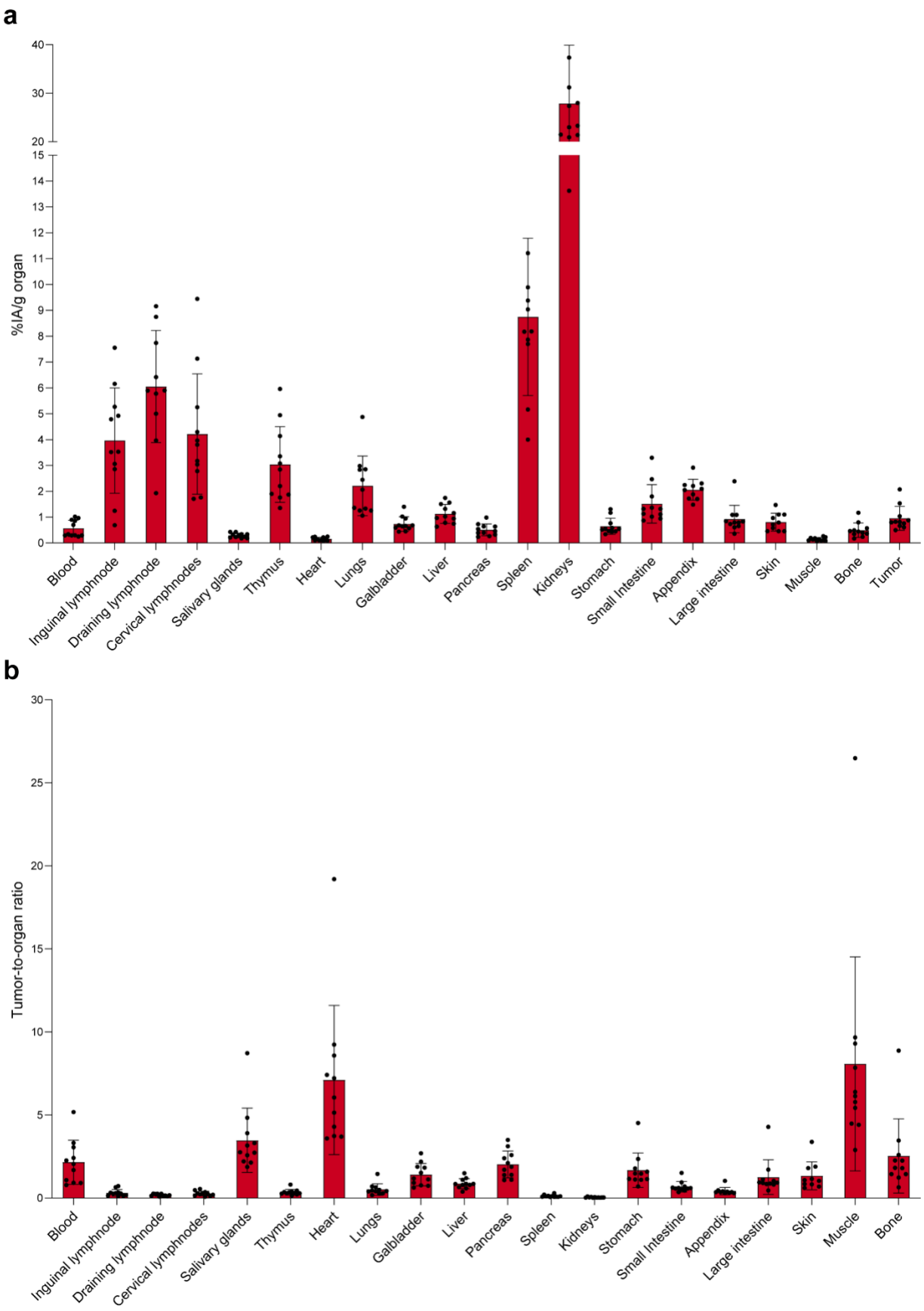
a
%IA/g organ
Blood
Inguinal lymphnode
Draining lymphnode
Cervical lymphnodes
Salivary glands
Thymus
Heart
Lungs
Galbladder
Liver
Pancreas
Spleen
Kidneys
Stomach
Small Intestine
Appendix
Large intestine
Skin
Muscle
Bone
Tumor
b
Tumor-to-organ ratio
Blood
Inguinal lymphnode
Draining lymphnode
Cervical lymphnodes
Salivary glands
Thymus
Heart
Lungs
Galbladder
Liver
Pancreas
Spleen
Kidneys
Stomach
Small Intestine
Appendix
Large intestine
Skin
Muscle
Bone

Supplemental Figure 9. Ex vivo biodistribution analysis of anti-human CD8β nanobody in MC38-tumor bearing human CD8 transgenic mice. *Ex vivo γ-counting (**a**) and tumor-to-organ ratios (**b**) of the isolated organs from MC38-tumor bearing human CD8-transgenic mice 80min after injection with [^{68}Ga]Ga-NOTA-anti-human CD8β nanobody. Biodistribution and tumor-to-organ ratios of the nanobodies in eleven mice are shown and expressed as mean ± SD of percentage of injected activity per gram of organ or tissue (%IA/g).*

Supplemental Table 1. *Overview of antibodies used for flow cytometry*

Target	Fluorophore	Species reactivity	Provider	Clone
CD11b	PE/Cyanine7	Human, Mouse	Biolegend	M1/70
His-tag	APC	/	Miltenyi Biotec	GG11-8F3.5.1
CD8	APC	Human	BD Bioscience	2ST8.5H7
CD8 Isotype control	APC	/	BD Bioscience	G155-178
CD69	APC	Human	Biolegend	FN50
CD4	PerCP/Cyanine5.5	Human	Biolegend	RPA-T4
CD4	PerCP/Cyanine5.5	Mouse	Biolegend	GK1.5
CD56	PerCP/Cyanine5.5	Human	Biolegend	QA18A21
CD3	FITC	Human	eBioscience	SK7
TCR beta	FITC	Mouse	eBioscience	H57-597
CD19	PE	Human	Biolegend	SJ25C1
CD19	PE	Mouse	eBioscience	1D3
CD45	APC/Cyanine7	Human	Biolegend	HI30
CD45	APC/Cyanine7	Mouse	Biolegend	30-F11
CD8	Brilliant violet 421	Human	Biolegend	RPA-T8
CD8	Brilliant violet 421	Mouse	Biolegend	53-6.7

Supplemental Table 2. Overview of the in vitro characteristics of the anti-human CD8β nanobody (hCD8β Nb). *Data are presented as mean ± S.D of at least 3 independent experiments.*

Nb	K_D hCD8αβ protein (nM) SPR	K_D SUP-T1 cells (nM) Flow cytometry	K_D hCD8αβ protein ELISA (nM)	K_D cynomolgus CD8β protein ELISA (nM)	Melting temperature (°C)
hCD8β Nb	1.0 ± 0.1	16.0 ± 9.0	2.4 ± 0.2	7.2 ± 1.4	68.1 ± 0.3

SPR: Surface plasmon resonance.

Supplemental Table 3. Radiochemical purity of radiolabeled anti-human CD8β or irrelevant nanobody. *The percentage of [^{99m}Tc]Tc- or [^{68}Ga]Ga-NOTA-anti-human CD8β nanobody (hCD8β Nb) or irrelevant nanobody (Irr Nb) after labeling (before purification) with ^{99m}Tc or ^{68}Ga and after purification. Data are presented as mean ± S.D of at least 3 independent experiments.*

Nb	^{99m}Tc RCP before purification (%)	^{99m}Tc RCP after purification (%)	^{68}Ga RCP before purification (%)	^{68}Ga RCP after purification (%)
hCD8β Nb	90.5 ± 6.5	99.8 ± 0.4	99.2 ± 0.3	99.4 ± 0.3
Irr Nb	92.7 ± 6.8	99.9 ± 0.1	98.6 ± 0.7	98.9 ± 0.8

RCP: Radiochemical purity

Supplemental Table 4. Overview of the in vitro characteristics of the NOTA-conjugated anti-human CD8β nanobody (hCD8β Nb). *Data are presented as mean ± S.D of at least 3 independent experiments.*

Nb	K_D hCD8αβ protein (nM) SPR	K_D SUP-T1 cells (nM) Flow cytometry
NOTA-hCD8β Nb	6.4 ± 2.1	9.3 ± 0.5

Supplemental Material and Methods

Cell culture

All cells were grown at 5% CO_2 and 37 °C. SUP-T1 cells were grown in Roswell Park Memorial Institute (RPMI) 1640 Medium (Gibco, Waltham, USA) supplemented with 1% Penicillin/Streptomycin (Gibco) and 10% Fetal Bovine Serum (FBS, Serana, Pessin, Germany). MC38 cells were grown in Dulbecco's Modified Eagle's Medium (DMEM, Gibco) supplemented with 1% Penicillin/Streptomycin and 10% FBS. Primary PBMCs were grown in Iscove's Modified Dulbecco's Medium (IMDM, Gibco) supplemented with 1% Penicillin/Streptomycin, 10% human AB serum (ZenBio, Durham, USA).

Nanobody generation and selection

Two llamas were subcutaneously injected 6 times with 100 µg recombinant human (h)CD8β-Avi-His_6 (U-Protein Express BV, Utrecht, The Netherlands) and 100 µg recombinant human CD8β-hIgG1 Fc (Sino Biological, Eschborn, Germany) mixed with Gerbu adjuvant P (Gerbu Biotechnik, Heidelberg, Germany) on a weekly basis. After immunizations, peripheral blood of both llamas was collected and peripheral blood mononuclear cells were isolated using lymphoprep tubes (Greiner Bio-one, Kremsmunster, Austria). RNA was isolated from peripheral blood lymphocytes using an RNA extraction kit (Qiagen, Hilden, Germany) and reverse transcribed into cDNA. Next, genes coding for the variable domain of the heavy-chain-only antibodies were amplified and ligated into the pMECS phage vector resulting in 2 separate phage display libraries. Subsequent biopanning was performed by infection of the libraries with M13K07 helper phages, resulting in phage production. For each library, 3 rounds of panning in solution were performed using in-house site-specifically biotinylated hCD8β-Avi-His_6 protein. For rounds 1 and 2, 100 nM antigen was used while 10 nM antigen was used during the final round of panning. In total, 190 unique clones (95 from round 2 and 95 from round 3) were randomly selected and screened for their ability to specifically bind to hCD8β by ELISA. Specific binding was determined by ELISA using site-specifically biotinylated hCD8β-Avi-His_6 protein, immobilized on a streptavidin-coated 96-well plate (Thermo Fisher Scientific). Positive hits were sequenced (Eurofins genomics, Ebersberg, Germany) and grouped into different B cell lineages based on the CDR3 sequence.

Surface plasmon resonance

The affinity of purified anti-hCD8β nanobody to recombinant hCD8αβ protein (Sino Biological) was determined using a Biacore-T200 device (Cytiva, Freiburg, Germany). The CD8αβ protein was immobilized on a CM5 chip (Cytiva) in 10 mM sodium acetate pH 4.5 using amine coupling chemistry to reach a final change in response units (RU) of 600 RU. Surface plasmon resonance measurements were performed at 25°C with HEPES-buffered saline (HBS, 10 mM of HEPES pH 7.4, 150 mM NaCl, 3.4 mM EDTA, 0.005% Tween-20) running buffer. The nanobody was injected sequentially, in a 2-fold serial dilution, starting from 0.98 to 250 nM at 30 µL/min. For each concentration cycle, an association step of 120 s was followed by a dissociation step of 600 s, a regeneration pulse of 60 s, using 100 mM glycine at pH 2.0, and a stabilization time of 180 s. For the single-cycle kinetics measurements, increasing concentrations of a 4-fold dilution of the nanobody, ranging from 0.49 to 125 nM, were consecutively injected for 180 s each, followed by a single dissociation phase of 600 s. After each binding cycle an identical regeneration pulse was performed followed by a stabilization period of 180 s. Local curve fitting analysis was performed using the Biacore evaluation software (Cytiva) by fitting the obtained sensorgrams to theoretical curves, assuming 1-1 binding geometries. For the determination of the equilibrium dissociation constant, the ratio of the association and dissociation rate constants was determined.

Immunofluorescence staining of non-human primate tissue

Lymph node tissues were fixed in Gerner buffer (0.1 M L-Lysine, 2 mg/mL $NaIO_4$, 4% formaldehyde and 0.05 M phosphate buffer) overnight at 4°C followed by dehydration in 30% sucrose for 24h. Next, samples were embedded in OCT mounting medium (VWR International, Radnor, USA) and frozen in liquid nitrogen-cooled iso-pentane. Tissue sections of 7 µm were cut using a Cryostat (Leica Biosystems) and mounted on SuperfrostPlus Gold glass slides (VWR International). Tissues were washed in wash buffer (0.05% Tween-20 in PBS) followed by incubation in permeabilization buffer (0.3% Triton X-100 in PBS) for 30 min at RT. Next, tissues were washed with PBS and incubated in blocking buffer (bovine serum albumin (BSA) in PBS) for 30 min at RT. Following another rinse step with PBS, tissues were incubated with saturation buffer (0.2% BSA in PBS) before overnight incubation at 4°C with Alexa Fluor-647 conjugated anti-hCD8β or irrelevant nanobody (10 µg/mL) and primary CD3 antibody (5 µg/mL;

Clone SP34.2, BD Biosciences) in Discovery Antibody diluent (Ventana, Roche). Subsequently, following a rinse with PBS and wash buffer, tissues were incubated with a Alexa Fluor-594-conjugated goat anti-mouse IgG1 secondary antibody (1 µg/mL diluted in Discovery Ab diluent; Invitrogen) for 4 hours at RT. Tissues were washed with wash buffer and fixed with 4% formaldehyde for 15 min at RT. Fixed tissues were repeatedly washed with PBS and stained with DAPI (1:50000 in PBS; Invitrogen) for 20 min at RT. Stained tissues were washed to remove excess dye and mounted with anti-fade mounting medium (ProLong Gold Antifade Mountant, Thermo Fisher) before being imaged using an automatic wide-field microscope (AxioScan Series 7, Zeiss).

Nanobody binding and T-cell activation assay using primary PBMCs

One day prior to the analysis, primary peripheral blood mononuclear cells were thawed and taken into culture. The next day, cells were resuspended in HBSS and 500000 cells were taken for each sample. Cells were stained with eBioscience Fixable Viability Dye eFluor 506 (1:1000 in HBSS; Thermo Fisher Scientific) for 30 min at 4°C. Cells were washed once with FACS buffer. Next, samples were incubated with human FcR blocking agent (Miltenyi Biotec, Bergisch Gladbach, Germany) diluted in FACS buffer according to manufacturer's protocol for 10min at 4°C. Next, 100 nM of anti-hCD8α (clone R3HCD27, patent US20190071500A1), anti-hCD8β or irrelevant nanobody were added for 1h at 4°C. Cells were washed once with FACS buffer and incubated with a mix of fluorescent antibodies (Table 1) for 30 min at 4°C. Cells were washed once again with FACS buffer before nanobody binding was determined. In case of the T-cell activation assay, 1 million cells were incubated with anti-CD3/CD28 dynabeads (Thermo Fisher) or 300 nM of GLP-grade anti-hCD8β or irrelevant nanobody for 24 h. The next day, cells were spun down and culture medium was collected. Secreted IFN-γ levels in the medium were determined using the human IFN-γ DUOset ELISA (R&D systems, Minneapolis, MN, USA) according to the manufacturer's protocol. Cells were stained with fluorescent antibodies (Table 1) for flow cytometry analysis as described above. Flow cytometry was performed using the FACS CANTO II analyser. Analysis was performed using FlowJo version 10.

^{99m}Tc-labeling of nanobodies

[^{99m}Tc]Tc-tricarbonyl was generated by the addition of 5.55 GBq [^{99m}Tc]TcO_4^- to the Isolink labelling kit (Paul Scherrer Institute, Villigen, Switzerland) for 20 min at 100°C. Next, 50 µg of His-tagged nanobody was added and incubated for 90 min at 50°C. ^{99m}Tc-labeled nanobodies were purified by gel filtration from the unbound [[^{99m}Tc]Tc$(H_2O)_3(CO)_3$]+ on a NAP-5 column (Cytiva) and filtered through a Millex 0.22 µm filter (Millipore, Haren, Belgium). The radiochemical purity of radiolabeled nanobodies was evaluated by instant thin layer chromatography (iTLC, Pall Corporation, Hoegaarden, Belgium)

SPECT/CT imaging and image analysis

Mice were injected i.v. with 5 µg of radiolabeled nanobody (± 37 MBq; 97.4 MBq/nmol (anti-hCD8β nanobody) or 108.8 MBq/nmol (irrelevant nanobody)). One hour after injection, mice were anesthetized with 75 mg/kg ketamine and 1 mg/kg medetomidine (Ketamidor, Richter Pharma AG, Weis, Austria) by intraperitoneal injection and SPECT/micro-CT imaging was performed using a Vector$^+$ scanner (MiLABS, Houten, The Netherlands). Imaging set-up consisted of a 1.5 mm 75-pinhole general-purpose collimator, in spiral mode with 6 bed positions. Total SPECT scanning time was 15 minutes with 150 seconds per position and CT scanning (60 kV and 615 mA) was 2 minutes. After imaging, mice were euthanized and organs were collected. Radioactivity in each organ was determined in a Wizard^2 γ-counter (Perkin-Elmer, Waltham, MA, USA). SPECT/CT image analysis was performed using AMIDE (UCLA, CA, USA) and OsiriX (Pixmea, Geneva, Switzerland) software.

NOTA-conjugation of nanobodies

The nanobody was first buffer-exchanged to 0.25 M sodium carbonate adjusted to pH 9.25 (sodium carbonate anhydrous; sodium hydrogen carbonate; sodium chloride, VWR Chemicals, Leuven, Belgium) using a PD-10 size exclusion column (Cytiva). A 20-fold molar excess of NOTA-NCS was added to the nanobody solution and incubated for 2h30 at RT. After incubation, the NOTA-nanobody was purified by size exclusion chromatography (SEC) on a Hiload 16/600 Superdex 30 pg column (GE Healthcare Bio-Sciences AB, Uppsala, Sweden) with 0.1 M NaOAc as the mobile phase (0.8 mL/min) to separate the conjugated nanobody from excess NOTA-NCS. The concentrations of the collected NOTA-nanobody fractions were measured spectrophotometrically using a Nanodrop 2000 device by UV absorption at 280 nm. In addition, SEC with a Superdex Peptide 10/300 GL column (GE Healthcare Bio-Sciences AB, Uppsala, Sweden) was performed for quality control of the NOTA-nanobody. The number of chelates per nanobody

was determined by electrospray ionization quadrupole time-of-flight mass spectrometry (ESI-Q-TOF-MS). After determining the chelator-to-nanobody ratio, anion exchange chromatography (AEX) was performed using an ENrich Q 5 × 50 column (Bio-Rad Laboratories, Inc., California, CA, USA) with 0.02 M Tris (VWR Chemicals, Leuven, Belgium) adjusted to pH 7.5 as solvent A and 0.02 M Tris with 0.31 M NaCl as solvent B (1.5 mL/min) to determine the fractions with different chelator-to-nanobody ratios. Based on these results, a 1:1 chelator-to-nanobody ratio was used for further radiolabeling.

^{68}Ga-labeling of nanobodies

The NOTA-conjugated nanobody (7.8 nmol for anti-hCD8β nanobody and 7.2 nmol for the irrelevant nanobody) was added to 1 mL of 1 M NaOAc buffer pH 5 and 1 mL of Gallium-68 (^{68}Ga) eluate (424-636 MBq) eluted from a ^{68}Ge/^{68}Ga generator in 0.1 M HCl (Galli Eo™, IRE ELiT, Fleurus, Belgium) and incubated for 10 min at RT. Purification was performed on a PD-10 desalting column pre-equilibrated with 1x PBS in case of the test-labeling or 0.9% NaCl containing 5 mg/mL vitamin C pH 5.8–6.1 (injection buffer) for stability and *in vivo* studies. After purification, the radioactive nanobody solution was filtered through a 0.22 µm filter (Millipore, Belgium). The radiochemical purity was assessed before and after purification by radio-iTLC ([^{68}Ga]Ga-NOTA-nanobody Rf = 0, [^{68}Ga]Ga-citrate Rf = 1). Radiometal chelation stability of the radiolabeled nanobody was assessed in different conditions (injection buffer (0.9%NaCl + 5 mg/mL Vitamin C) at RT or 37°C; human serum at 37°C) at 30min, 60min, 120min and 180min after labeling. Stability of the radiolabeled compound was analyzed by radio-iTLC and radio-SEC at these timepoints.